Study of Air Flow Around a Moving Vehicle as a Source of Energy

Dalibor Barta[(✉)] , Vladimir Pavelcik , and Milos Brezani

University of Žilina, Univerzitna, 8215/1, 010 26 Žilina, Slovakia
{dalibor.barta,vladimir.pavelcik,
milos.brezani}@fstroj.uniza.sk

Abstract. The growing number of vehicles is related to the overall growth in the consumption of fuel from fossil fuels or electricity, so new ways are being sought to increase the efficiency of propulsion or the recovery of energy from driving. This article deals with the possibility of recovering kinetic energy from the movement of vehicles, specifically from the air flowing around a passing car. The subject of measurements and simulations were parameters influencing the amount of recovered energy such as the location of the wind turbine near the road, its distance from the side of the moving vehicle, turbine height from the road, speed and size of the vehicle front (car, bus, truck). The measured values were compared with the values from the simulations performed in the program Fluent, and it was shown that in passenger cars the highest air flow is 0.5–1 m above the road and the closest possible to vehicles. With regard to feasibility, the smallest distance was considered to be 0.5 m from the side of the vehicle. Measurements in real traffic showed delay of the air flow behind the vehicle by 1.5–3 s depending on the size of the vehicle and the need for sufficient traffic density. The high intensity of vehicles in urban and suburban areas predestines them to deploy this system. Conversely, in rail transport, given the low frequency of vehicles, the use of this system is unjustified.

Keywords: Vehicle · Airflow · Energy recuperation · Vehicle distance

1 Introduction

Modern society is very energy intensive. It makes extensive use of fossil fuels in transport, and therefore considerable pressure is being exerted to increase the efficiency of propulsion and, if possible, to reuse propulsion energy. In order to reduce the amount of energy required, research into new, lighter materials is underway [1] and the driving characteristics of vehicles are being optimized [2]. In internal combustion engines, where only about one third of the energy stored in the fuel is converted into efficient engine power, the rest goes mainly to the cooling and exhaust system [5], conventional fossil fuels, whose combustion products have a serious impact on the environment, are replaced by alternative [3, 4]. In order to meet the ever-tightening emission standards, several strategies have been developed over time. One of them is the change of the type of propulsion unit from an internal combustion engine to an electric motor, the efficiency of which is much higher than the efficiency of the internal

combustion engine and in which no gaseous emissions are produced locally. The advantages of both types of drives, sufficient range, the ability to achieve local zero emissions, or the ability to recover energy from braking, are provided by their combination in hybrid vehicles [6–8]. According to Jinglai et al. [9], in the hybrid drives the electric motors with internal combustion engines can be connected to wheels in different ways, some of which are more efficient than others.

There are many ways to recover energy in vehicles. Some of them are described below. Closer attention will be paid to the possibilities of obtaining energy from the air flowing around the oncoming vehicle and its conversion into electrical energy. Not much attention has been paid to this topic so far, so CFD simulations and real measurements in operation were performed, which showed what has a significant impact on the amount of energy obtained.

2   Energy Recovery

2.1   Braking Energy Recovery

Various energy recovery systems have been designed to make more efficient use of the energy supplied in the fuel and thus to further reduce the total energy wasted by the vehicle. These systems are based on different physical principles (Fig. 1), which aim to convert as much of the kinetic energy of the vehicle as possible to some other usable form instead of converting it to heat in the disc brake.
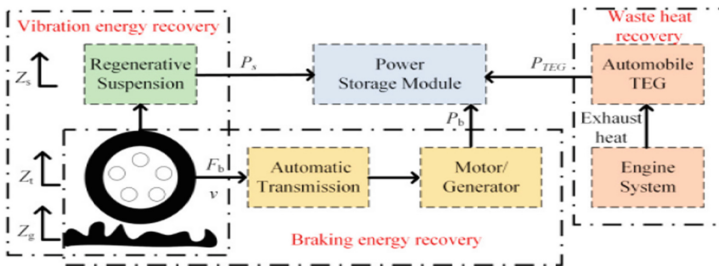
Fig. 1. General architecture of the comprehensive vehicle energy recovery system [10].

Electrical system of recuperation uses the drive motor itself switched to the generator mode. The generator then feeds the battery with the resulting current. This braking effect can be used only on driving wheels. Guo et al. [11] discussed the importance and effect of strategy of braking force distribution in such case. With the progress in optimization theories, more braking energy changing algorithms (intelligent neuro-fuzzy systems, such as proposed by Medvedev and Rudakov [12]) have been developed in order to maximize recuperated energy. On top of algorithms, whole strategies have been developed, based on the vehicle mass and road parameters (Boisvert et al. [13]) or based on the number of driven wheels (four-wheel independent drive strategy proposed by Li et al. [14]). Energy recovery strategy based on pedals

positions of electric vehicle suggested by JI et al. [15] extended driving range of electric vehicle by more than 20% when compared with the mode of no energy recovery. A genetic-fuzzy control method proposed by Liu et al. [16] was proven to increase the recoverable energy ratio by 2.7% compared to model before optimization.

The electric recuperation system is the most common recuperation system used in vehicles. It uses the drive motor itself switched to generator mode for deceleration. The generator generates braking torque in the production of electricity. The obtained electrical energy then powers the battery. This braking effect can only be used on the drive wheels. Guo et al. [11] discussed the importance and effect of a brake force distribution strategy in such a case. With advances in optimization theories, several algorithms have been developed to change the braking energy (intelligent neurofuzzy systems as proposed by Medvedev and Rudakov [12]) in order to maximize the energy recovered. In addition to algorithms, whole strategies have been developed based on mass and traction parameters (Boisvert et al. [13]) or on the number of driven wheels (an independent all-wheel drive strategy proposed by Li et al. [14]). An energy recovery strategy based on the pedal positions of an electric vehicle proposed by JI et al. [15] can extend the range of an electric vehicle by more than 20% compared to the mode without energy recovery. The genetic fuzzy control method proposed by Liu et al. [16] demonstrably increased the usable energy ratio by 2.7% compared to the model before optimization.

Mechanical system of recuperation uses flywheels in two configurations. First of them is purely mechanical, where the kinetic energy is transferred from wheel into flywheel during braking and is returned to wheel during acceleration. Second one is electro-mechanical, where energy from wheels is converted in generator/motor into electric energy, but instead of battery, electricity is stored via motor/generator in flywheel. Flywheel can be used in vehicle without electric engine as well as in hybrid vehicles, where energy accumulated in flywheel can be converted into electricity and stored in battery. Summary of energy recovery technology was made in detail by Fahlbeck and Kindahl [17]. Minimizing losses in flywheel system is a matter of decreasing friction and storing the flywheel in vacuum.

Hydraulic recuperation is based on accumulating energy in pressurized gas. The gas is pressurized by hydraulic pump pumping hydraulic liquid into bladder accumulator during braking. Energy is then used to propel the car with hydraulic engine powered by expanding gas. There are more concepts, however, mostly operating on the same principle. The main disadvantage of this system is its weight and dimensions, thus its useability in casual cars is limited. On the contrary, according to Schwalbe et al. [18], strongly influenced by the velocity profile, the energy consumption savings can reach up to 74% for harmonic sinusoidal profile.

2.2 Waste Heat Recovery

In internal combustion engine, about 30% of energy stored in fuel is exhausted through exhaust pipe. Some part of this energy can be recuperated using thermoelectric materials. Thermoelectric generator is made of couples of thermoelectric legs thermally connected in parallel and electrically in series. The generated electrical power is given by the amount of heat and effectivity of the generator. Durand et al. [19] have shown in

the study that the amount of heat is directly affected by position of the generator (Fig. 2) (the energy generated after the exhaust of after-treatment system (ATS) is 5 times lower when compared to the position before turbocharger). At higher engine loads, about 150 W can be expected to be generated this way.
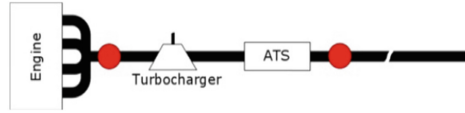

Fig. 2. Investigated locations of thermoelectric generators [19].

2.3   Vibration Energy Recovery

Because damping is essential part of any vehicle, there have been some experiments with collecting as much of the energy wasted in dampers as possible. At present, active shock absorbers are already in use, which make it possible to obtain energy when the vehicle passes over uneven ground. Caban et al. [20], for example, dealt with the issue of possibilities of energy harvesting from the engine mount damping system of the vehicle. For instance, rack-pinion damper aims to convert damped motion into rotation of motor/generator via gear rack and gear box, however, this system is subject to greater losses in efficiency. Average power output of this system was 19 W per damper when tested on relatively smooth road [21].

There are other recuperation concepts using damping, such as damping of linear movements, hydraulic electromagnetic damping, damping of ball screws, etc. [17], but a detailed overview of them is beyond the scope of this article.

2.4   Energy Recovery on the Road

Zahibi and Saafi [22] reviewed current possibilities of collecting energy from road infrastructure. In the article, piezoelectric, thermoelectric, photovoltaic, and electro-magnetic energy harvesters are compared using method proposed by Clausing and Holmes [23]. According to their results, electromagnetic technology tops all other in power output, however, it influences the traffic flow. Photovoltaic systems power output is highly dependent on weather conditions and its initial costs as well as maintenance are relatively high. Both thermoelectric and piezoelectric systems are easy to install, but they provide very low power output at expensive initial costs.

3   Wind Energy Recovery

As has already been mentioned, energy is consumed to accelerate and move the vehicle. However, the vehicle acts on its surroundings and, for example, sets the ambient air in motion. The vehicle transmits kinetic energy into the air, which can later be captured by wind turbines and used to generate electricity. In order to design a wind

turbine to convert energy from traffic and to evaluate the velocity of the air that drives the turbine, a CFD simulation was performed.

In order to know the real air velocities at different locations near the oncoming vehicle, experiments were performed in real traffic. The experiments also made it possible to determine the approximate distance between successive vehicles, i.e. the frequency of vehicles at which the rotation of the turbine would not be stopped. The measurements were made in two locations in and around Žilina city, with the speed limits of 70 and 90 km·h^{-1} respectively, generally well representing ratio of number of smaller cars to number of SUVs and of trucks and busses. Both mechanical and electrical anemometers intended for meteorological purposes were used to measure the speed of the air and its direction. Horizontal distance was measured between anemometer and vehicle's right wheels.

The results in Table 1 show that smaller vehicles tend to drive more from the roadside than larger vehicles. However, the difference is roughly correlated with the difference in the average widths of these vehicle types. The values of the distance of the vehicle from the measuring point were influenced by the fact that drivers have a natural tendency to avoid a place on the road where a person is located (measuring point). However, it can be assumed that the wind turbine itself located near the track will not affect the behavior of the drivers and thus it will be possible to place it closer to moving vehicles.

Table 1. Comparison of distance between various vehicle types and the anemometer.

| Vehicle type	Average measured distance [m]
Smaller cars	1.99
SUV	1.77
Trucks, buses	1.65
Total average	1.8

A CFD simulation was performed in the ANSYS Fluent program, the aim of which was to reveal the direction of air flow around the vehicle after passing the measuring point, so that the turbine could be positioned as best as possible in terms of direction and speed of air flow. A coordinate system was used where the positive values on the x-axis are in the road plane and against the direction of travel, the y-axis is perpendicular to the x-axis in the road plane and the z-axis is vertical. The starting point of the coordinate system is at the rear of the vehicle. According to Hamat et al. [24], although the situation is a complex transition problem, considerable simplification can be made to reduce computational time. The simulation settings are summarized in Table 2.

The model of the vehicle was derived from a CAD model of Opel Zafira. Because rear view mirrors contribute to aerodynamic drag of the vehicle in considerable way, (causing turbulences), the velocity magnitudes are expected to be higher in reality.

Table 2. Simulation settings.

Geometry	Simplified CAD model of Opel Zafira (without wheels and rear-view mirrors)
Fluid domain dimensions	Distance before the vehicle - lengths of 4 vehicles (VL), above the vehicle - 3 VL, next to the vehicle - 3 VL, distance behind the vehicle - 16 VL
Mesh	Overset mesh applied near the vehicle Polyhedral elements Symmetry applied
Mesh quality	$1.2.10^6$ cells, minimum orthogonal quality 0.558, maximum aspect ratio 53.7; y^+ according to turbulence model requirements
Turbulence model	k-ε realizable
Solver	Coupled
Steady-state simulation	Yes, inlet velocity 25 m·s^{-1}

Steady-state simulation could have been made because of interest only in velocity fields around the vehicle (Fig. 3). To compensate the simplification of constant inlet velocity, the initial velocity was subtracted from the velocity v_x (in the vehicle movement direction). The velocity v_x, the velocity v_y (in the direction perpendicular to the vehicle movement and in the horizontal plane) and their combination magnitude in the distance of 180 cm away from the vehicle (selected according to the measurement) in different height levels above the ground are displayed in the Fig. 4 ($\underline{v_x}$), Fig. 5 ($\underline{v_y}$) and in the Fig. 6 (comparison of them).
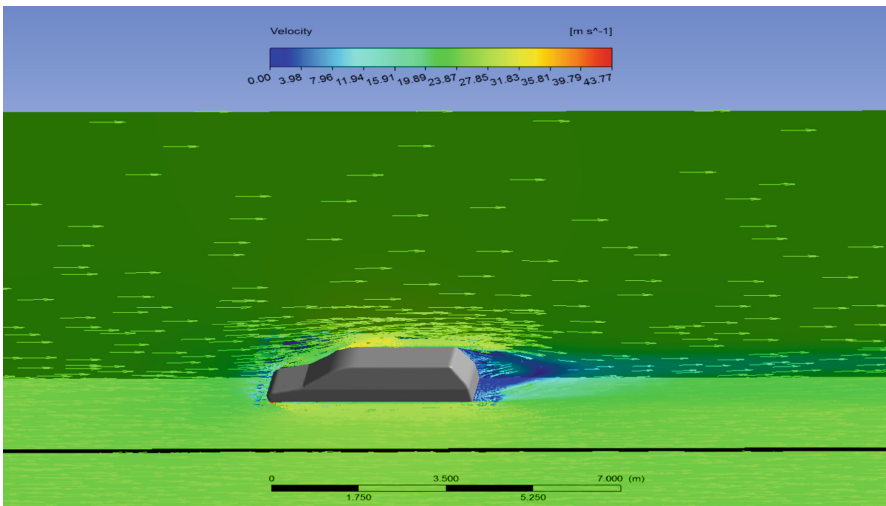

Fig. 3. Relative velocity vectors (black line is 1.8 m away from the vehicle).
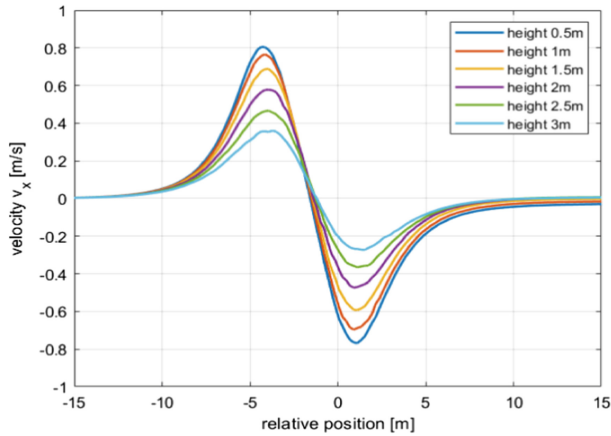
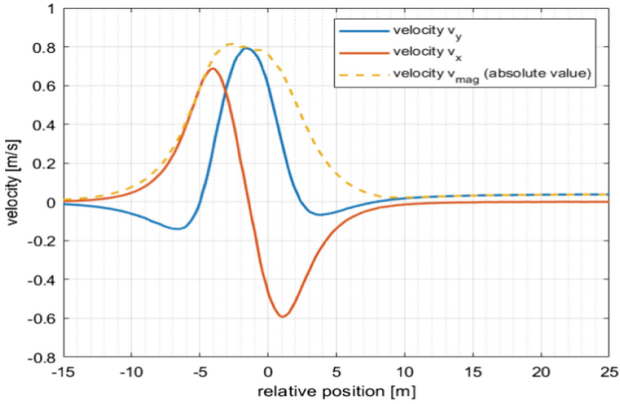**Fig. 4.** Comparison of velocities v_x in different heights.

The curves in the Fig. 4 show the size of components x of the air velocity vectors (horizontal axis is parallel to the 'x' direction). The first peak values are achieved approx. 4 m before the rear end of the vehicle (which means this peak is located at the front end/near front wheels), the second peak ca. 1 m behind the vehicle. The change from positive to negative values indicate the change of direction of this vector component. Similarly, in the Fig. 5, the size of components y of the air velocity vectors is presented (horizontal axis represents the same line as in the Fig. 4). The peak value is now in the location corresponding to the front door of the vehicle. In both cases, the biggest peak values are observed in the height 0.5 m to 1 m over the road.
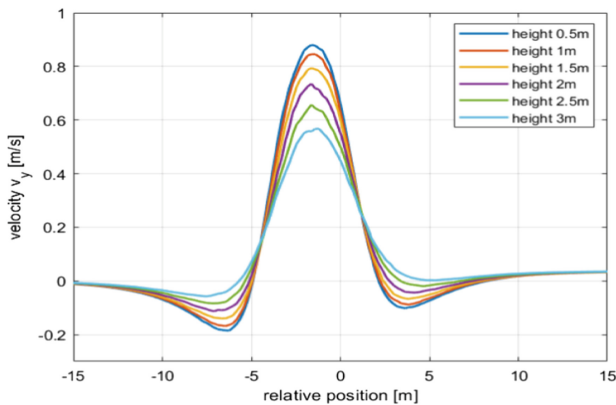
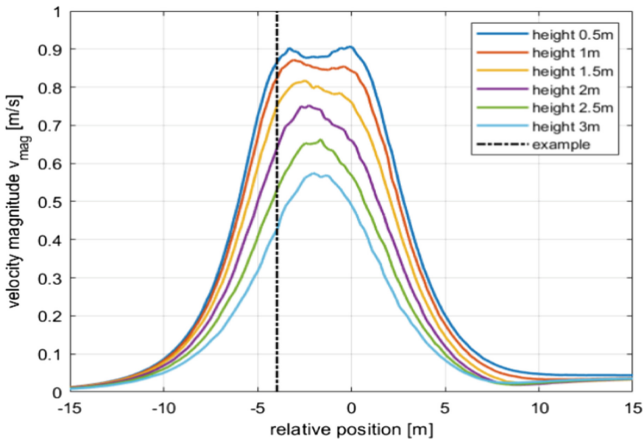**Fig. 5.** Comparison of velocities v_y in different heights.

The resulting velocity magnitude v_{mag} presented in the Fig. 6 is obtained from velocities v_x and v_y via following equation:

$$v_{mag} = \sqrt{v_x^2 + v_y^2}. \tag{1}$$

Fig. 6. Comparison of velocity profiles at height 1.5 m above the ground.

Resulting velocity magnitudes in different height levels are compared in the Fig. 7. Vertical part of velocity vector is omitted, because this part of the vector is not able to propel the vertical axis wind turbine without curved blades.


Fig. 7. Comparison of velocity magnitudes at different height levels.

With increasing height, the velocity magnitude changes. The decrease of the velocity magnitude is showed in the Fig. 8. Hereby a conclusion can be made, that by decreasing the distance between the turbine and the ground from 1.5 m to 1 m can

increase velocity magnitude by 6.6% (in reality, this could be higher, because of the simplifications applied to the simulation model).
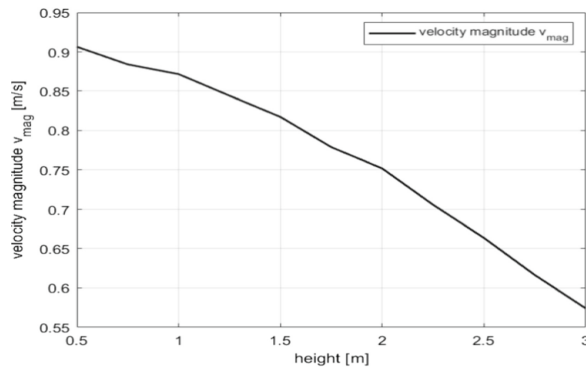
Fig. 8. Effect of height on the velocity magnitude xy.

The effect of changing the distance between the vehicle and the turbine is demonstrated in following figures by one example. The position of the measuring point for which the calculation was made is shown in Fig. 7 by a black dashed line. It is the position where the velocity v_x reaches its maximum and the velocity magnitude is close to its local maximum.

Figure 9 shows the course of the speed as a function of the changing distance of the vehicle from the turbine. As can be seen, moving the turbine 20 cm closer (from the distance 1.8 m) to the vehicle (or the vehicle closer to the turbine) results in a 13% increase in air velocity and thus an increase in turbine power.
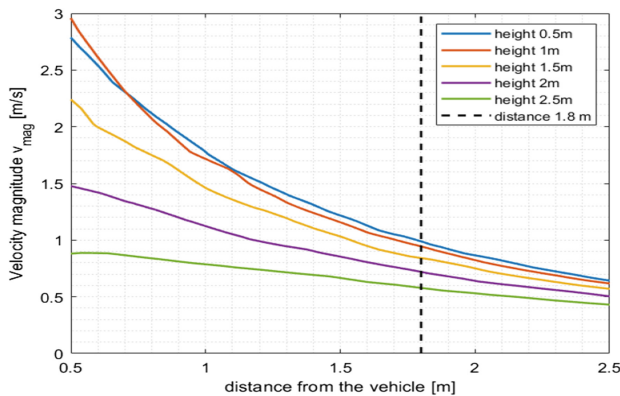
Fig. 9. Effect of increasing distance from the vehicle on velocity magnitude.

The power P_w, which can be passed by wind to an object, is given by the formula [26]:

$$P_w = \frac{1}{2} \cdot A \cdot \rho \cdot v^3, \qquad (2)$$

where A is the projected area (of a blade), ρ is density of air and v is velocity of air. This formula shows the importance of correct placement of the wind turbine, because even small addition to the velocity is powered by 3. The simulation was verified by the above-mentioned measurements. Air velocity magnitude induced by smaller vehicles reached up to 1–2 m·s^{-1}, SUVs and smaller vans up to 4.5 m·s^{-1} and buses and trucks up to 7 m·s^{-1}. These values are average, as their size can be influenced by the shape of the vehicle body, the speed limit on the road and also by the wind from the surroundings, even if the measurements were made in windless or light breeze. Savonius turbine or Banki rotor are considered the best choices for such a case, because of only low velocity needed to start their rotation. The difference between them and their comparison for similar case is summarized by Tian et al. [25]. However, these turbines have only small efficiency (about 15%), so the power output P_t of the turbine can be estimated as [25]:

$$P_t = 0.15 \cdot P_w. \qquad (3)$$

The power output for whole day can then be calculated by statistically counting vehicles and their types (taking into account different wind velocity magnitudes of different types of vehicles). The whole methodology is proposed by Penne et al. [26].

Because of the effect shown in previous figures, the easiest way to maximize the power output of a wind turbine is to move it closer to the vehicle. This can be hardly achieved on a highway, where the dimensions and no-obstacle-spaces are strictly given by local rules. However, there is a possibility to move the turbine closer to vehicle on the roads in the city. The width of such roads is smaller, the roadside is nearer to the vehicle. Even though vehicle drive at lower speed, there are road sections in the cities, where speed limit is 70 km·h^{-1} or even higher, where potential of this system could be used successfully. Another possibility for this system would be to collect the wind energy generated by rail vehicles. A single train, due to its length, can provide longer-lasting "impulse", probably of higher velocity (the turbine can be placed in smaller distance from the train), however, the frequency of trains could be too low to keep this system efficient.

In general, the effect of the turbine on the vehicle and its aerodynamic drag is estimated to be negligible, but further research is needed for confirmation.

4   Conclusion

There are many options for recovering energy from driving. Measurements in real traffic as well as simulations performed in the Fluent program have shown that it also has the potential to capture wind energy generated by driving the vehicle around wind

turbines located near the road. As it is shown in simulation results, side effect of overcoming air resistance is arising of airflow around the vehicle. For example, near the front part of the simulated car, in the distance of 0.5 m, velocity magnitude can reach up to 3 m·s^{-1}, decreasing with increasing distance from the vehicle to 1 m·s^{-1} at 1.8 m away from the vehicle. Velocity magnitude is also influenced by height between the measured place and the road level, and by aerodynamic parameters as well. As shown the measurements in real traffic, the increment of velocity magnitude provided by vans, trucks and buses was significant.

Interesting values have been measured behind the vehicles. Average velocity of all types of vehicles was ca. 4 m·s^{-1} and was measured 1 s after the vehicle passed by the measurement setup. For trucks with semi-trailers, this could reach up to 7 m·s^{-1} and 3 s behind the vehicle. Taking into account the complexity and time-consumption of transient simulation of such case in Fluent, it will be interesting to further focus on this problematic and to implement the influence of climatic conditions and surrounding environment on the velocity magnitude. Placement, type and dimensions are the next part of solution of effective usage of this source of wind energy. The study has demonstrated the importance of suitable placement of wind turbines from the power-maximization point of view. To keep the rotation of the turbine – generator system, sufficiently dense traffic is needed (around 1 vehicle per second) with speed above 50 km·h^{-1}. Given requirement denies the possibility of using this principle on railways. Even though a higher amount of energy can be collected from a single train, the distance between trains (and in a conclusion low frequency) does not make this solution effective. Due to significant decrease of air velocity with increasing distance from vehicle, the usability of this system could be constrained on the highways with wide emergency lane. For further research, placement of turbines between fastest lines could be considered, where although the frequency of vehicle is lower, they tend to drive faster, and the turbine could be propelled by vehicles on both sides. Analysis results show estimation of effective usage of this system in city traffic ideally on four-lane roads with high density of vehicles moving at velocity higher than 50 km·h^{-1} with wind turbines installed in between lanes of opposing direction as well as near the roadsides. Of course, with the use of turbines in the vicinity of moving vehicles, the question arises as to what extent their presence may affect traffic safety. However, it can be assumed that their influence should not be higher than the influence of barriers. And since their use proves to be advantageous only in certain places, these can be labeled.

References

1. Blatnicky, M., Saga, M., Dizo, J., Bruna, M.: Application of light metal alloy EN AW 6063 to vehicle frame construction with an innovated steering mechanism. Materials **13**(4), 817 (2020)
2. Dizo, J., Blatnicky, M.: Investigation of ride properties of a three-wheeled electric vehicle in terms of driving safety. Transp. Res. Procedia **40**, 663–670 (2019)
3. Lebedevas, S., Pukalskas, S., Žaglinskis, J., Matijošius, J.: Comparative investigations into energetic and ecological parameters of camelina-based biofuel used in The 1Z diesel engine. Transport **27**(2), 171–177 (2012)
4. Korsakas, V., Melaika, M., Pukalskas, S., Stravinskas, P.: Hydrogen addition influence for the efficient and ecological parameters of heavy-duty natural gas si engine. Procedia Eng. **187**, 395–401 (2017)
5. Caban, J., Drozdziel, P., Ignaciuk, P., Kordos, P.: The impact of changing the fuel dose on chosen parameters of the diesel engine start-up proces. Transp. Prob. **14**(4), 51–62 (2019)
6. Pukalskas, S., et al.: Comparison of conventional and hybrid cars exploitation costs. Adv. Sci. Technol. Res. J. **12**(1), 221–227 (2018)
7. Małek, A., Caban, J., Wojciechowski, L.: Charging electric cars as a way to increase the use of energy produced from RES. Open Eng. **10**(1), 98–104 (2020)
8. Brumercik, F., Lukac, M., Caban, J.: Unconventional powertrain simulation. Commun. Sci. Lett. Univ. Zilina **18**(2), 30–33 (2016)
9. Jinglai, W., et al.: Efficiency comparison of electric vehicles powertrains with dual motor and single motor input. In Mechanism and Machine Theory. **128**, 569–585 (2018)
10. Wei, Y., Ruochen, W., Runze, Z.: A Comparative research on the energy recovery potential of different vehicle energy regeneration technologies. Energy Procedia **158**, 2543–2548 (2019)
11. Guo, J., Wang, J., Cao, B.: Study on braking force distribution of electric vehicles. In: Proceedings of Asia-Pacific Power and Energy Engineering Conference, Wuhan, China, pp. 1–4 (2012)
12. Medvedev, V., Rudakov, I.: Self-adaptive algorithm for changing braking energy recuperation of an electric vehicle based on neuro-fuzzy inference system. In: Proceedings of IASF - Technologies and Components of Land Intelligent Transport Systems, Moscow, Russia (2019)
13. Boisvert, M., et al.: Comparison of two strategies for optimal regenerative braking, with their sensitivity to variations in mass, slope and road condition. IFAC Proc. **46**(21), 626–630 (2013)
14. Li, L., et al.: Energy recovery strategy for regenerative braking system of intelligent four-wheel independent drive electric vehicles. IET Intell. Transp. Syst. **15**, 119–131 (2021)
15. Jl, F.Z., et al.: Energy recovery based on pedal situation for regenerative braking system of electric vehicle. Veh. Syst. Dyn. **58**(1), 144–173 (2020)
16. Liu, Z.Q., Lu, S., Du, R.H.: A genetic-fuzzy control method for regenerative braking in electric vehicle. Int. J. Comput. Sci. Math. **11**(3), 263–277 (2020)
17. Fahlbeck, J., Kindahl, J.: Energy recovery systems in cars and detail study of flywheel regenerative braking systems. Bachelor thesis, Chalmers University of technology, Gothenburg, Sweden (2016)
18. Schwalbe, K., et al.: Recuperation gain for a hydraulic energy storage in automotive applications. Appl. Thermal Eng. **175**, 115275 (2020)
19. Durand, T., et al.: Potential of energy recuperation in the exhaust gas of state of the art light duty vehicles with thermoelectric elements. Fuel **224**, 271–279 (2018)

20. Caban, J., Litak, G., Ambrożkiewicz, B., Gardyński, L., Stączek, P., Wolszczak, P.: Possibilities of energy harvesting from the suspension system of the internal combustion engine in a vehicle. Commun. Sci. Lett. Univ. Zilina **23**(2), 106–116 (2021)
21. Li, Z., et al.: electromagnetic energy-harvesting shock absorbers: design, modeling, and road tests. IEEE Trans. Veh. Technol. **62**, 1065–1074 (2013)
22. Zahibi, N., Saafi, M.: Recent developments in the energy harvesting systems from road infrastructures. Sustainability **12**(17), 6738 (2020)
23. Clausing, D., Holmes, M.: Technology readiness. Res. Control Manag. **53**, 52–59 (2010)
24. Hamat, A.M.A., Kahar, O., Md, N.M.: Renewable energy from induced airflow generated by cruising ground vehicles in tandem using RANS. Energy Procedia **14**, 1877–1882 (2012)
25. Tian, W., Song, B., Mao, Z.: Numerical investigation of wind turbines and turbine arrays on highways. Renew. Energy **147**(1), 384–398 (2020)
26. Penne, M., Qiao, W., Hudgins, J.: Converting waste vehicle aerodynamic energy into electricity. In: IEEE Energy Conversion Congress and Exposition (ECCE), pp. 416–422 (2018)